EACS 2016 – 6th European Conference on Structural Control Sheffield, England: 11-13 July 2016
Paper No. 155

EXPERIMENTAL STUDY OF THE EFFECTIVENESS OF SEMI-ACTIVELY IMPLEMENTED POWER-LAW DAMPING ON SUPPRESSING THE SEISMIC RESPONSE OF A BASE-ISOLATED BUILDING

Maki DAN[1*], Masashi OMURA[2], Fumito NAKAMICHI[3], Masayuki KOHIYAMA[4], & Zi-Qiang LANG[5]

[1,2,3,4]*Graduate School of Science and Technology, Keio University, Hiyoshi 3-14-1, Kohoku-ku, Yohokohama-shi, Kanagawa, Japan*
[5]*Department of Automatic Control and Systems Engineering, The University of Sheffield, Mappin Street, Sheffield, United Kingdom*

E-mail address of corresponding author*: maki.dan@keio.jp

ABSTRACT. This study focuses on verifying the effectiveness of the nonlinear power-law damping system on reduction of the vibration of base-isolated buildings with semi-actively implemented dampers over the ranges of resonance frequencies without causing detrimental effects over other frequency ranges. To verify the effectiveness of the proposed power-law damping system, shaking-table tests on a small-scale two-story physical building model are conducted. Random ground motions are used as the input excitations. The physical building model is equipped with a semi-active oil damper whose damping coefficient can be varied over four different values. This provides an effective mechanism for semi-actively implementing the power-law damping system. The shaking-table tests have demonstrated the effectiveness and robustness of the power-law damping and indicated that this can be a more practical solution to improving the performance of building base-isolation systems.

KEYWORDS: *base-isolated building, semi-active oil damper, power-law damping, shaking-table test*

1 INTRODUCTION

Traditionally, base-isolation systems for buildings are designed based on the principle of shifting the structural resonance frequencies to a frequency range that is well below the dominant frequencies of earthquake ground motion. Although these systems have worked well, the 2011 Tohoku earthquake, which was the largest earthquake recorded in Japan, revealed the importance to prepare for the rarely occurring long-period waves. This is because a high-rise building, which was built to have a long natural period, suffered damage due to the long-period waves of the 2011 Tohoku earthquake.

In order to improve the performance of base-isolation systems, semi-active oil dampers have been widely used as actuators to implement different control actions. These techniques are based on the principle of active vibration control that often relies on an accurate model of the building structure which is difficult to be determined in practice. However, the recent study which analyzed vibration records of a semi-active base-isolated building before, during, and after the 2011 Tohoku earthquake, revealed that the vibration characteristics of base-isolated buildings would change due to earthquake excitations [1]. To overcome this problem, in this study, we propose to introduce nonlinear power-law damping and to implement a designed power-law damping characteristic using a semi-actively controlled damper. Conventional linear damping can reduce the building response over the range of structural resonance frequencies. However, at the same time, it has detrimental effects on the vibration suppression over higher frequency ranges., Previous studies (e.g. [2] and [3]) have suggested that the nonlinear power-law damping has potential to significantly suppress the vibration over the ranges of resonance frequencies without causing detrimental effects over other frequency ranges. This implies that a properly designed power-law damping can potentially achieve an effective base-isolation not only for more frequent earthquakes but also for the long-period waves from rarely occurring earthquakes like the 2011 Tohoku earthquake.

To verify the effectiveness of the proposed power-law damping system, shaking-table tests on a small-scale two-story physical building model are conducted. Random ground motions are used as the input excitations. The building model was designed such that the ratio between first and second natural periods is the same as that of a target real scale base-isolated building. In addition, the physical building model is equipped with a semi-active oil damper whose damping coefficient can be varied over four different values. This provides an effective mechanism for semi-actively implementing the power law damping system. The shaking-table tests have demonstrated the effectiveness and robustness of the power-law damping and indicated that this can be a more practical solution to improving the performance of building base-isolation systems.

2 EXPERIMENTAL SETUP

2.1 Design of the specimen

A small-scale specimen is designed to physically simulate a base-isolated building with semi-active oil dampers. Figure 1 (a) shows the specimen with a semi-active oil damper. To represent the characteristics of base-isolated building, aluminum material, which is a light weight material, is used for the columns of the first floor. Other parts of the specimen are made of stainless steel material. Fig. 1 (b) shows the model of the specimen. Here, m_i, c_i, k_i, and x_i ($i = 1, 2$) represent the mass, damping coefficient, stiffness, and displacement of the i-th floor, respectively. In addition, c_3 represents the damping coefficient of the semi-active oil damper

and $\ddot{x}_0$ represents the absolute acceleration of the ground motion. The mass matrix $\mathbf{M}$ is given as

$$\mathbf{M} = \begin{bmatrix} m_1 & 0 \\ 0 & m_2 \end{bmatrix} = \begin{bmatrix} 3.264 & 0 \\ 0 & 1.589 \end{bmatrix} \text{kg}. \tag{1}$$

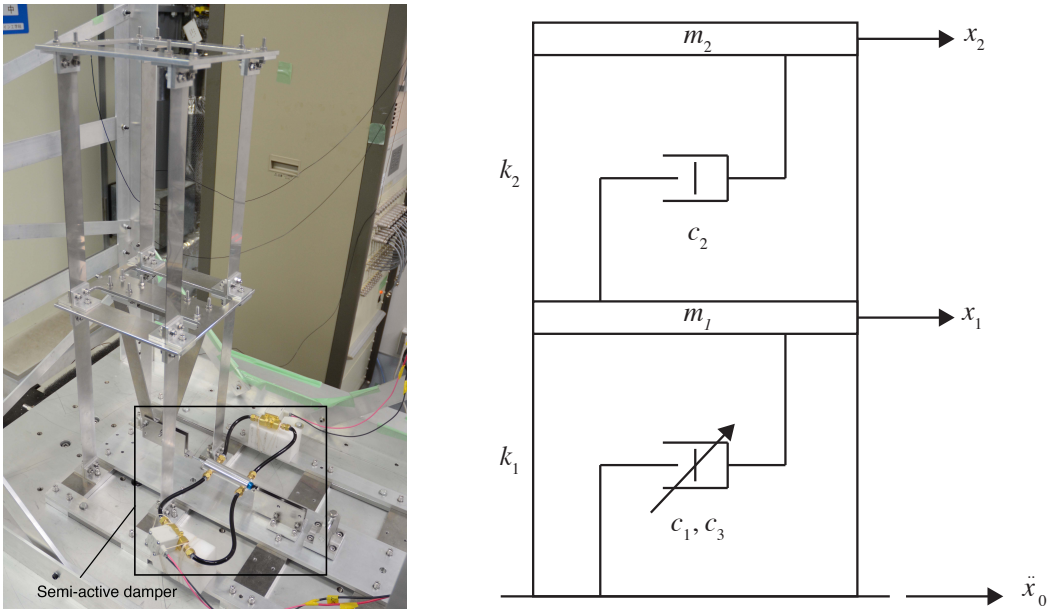

(a) Photo of the specimen (b) 2-DOF model

Figure 1: Design of specimen with a semi-active oil damper

With the mass matrix being known apriori, system identification is conducted through a free vibration experiment and the natural periods of the first and second mode and damping ratio are obtained from the measurement of the acceleration sensors attached to each floor. Results of the system identification are shown in Table 1. By using the values of Table 1 and measured mass matrix $\mathbf{M}$, the identified stiffness matrix $\mathbf{K}$ is calculated as

$$\mathbf{K} = \begin{bmatrix} k_1 + k_2 & -k_2 \\ -k_2 & k_2 \end{bmatrix} = \begin{bmatrix} 2.22 & -1.97 \\ -1.97 & 1.97 \end{bmatrix} \times 10^3 \text{N/m}. \tag{2}$$

Assuming a proportional stiffness damping, the damping matrix $\mathbf{C}$ is given in equation (3) in which T_1 and $zeta_1$ are the natural period and the damping coefficient of the first mode shown in Table 1, respectively.

$$\mathbf{C} = \frac{2\zeta_1 T_1}{2\pi}\mathbf{K} \tag{3}$$

From equation (3), the damping matrix $\mathbf{C}$ is calculated as

$$\mathbf{C} = \begin{bmatrix} c_1 + c_2 & -c_2 \\ -c_2 & c_2 \end{bmatrix} = \begin{bmatrix} 1.15 & -1.02 \\ -1.02 & 1.02 \end{bmatrix} \text{Ns/m}. \tag{4}$$

Table 1: Results of system identification

Parameter	Value
Natural period of the first mode T_1	0.882 s
Natural period of the second mode T_2	0.145 s
Damping coefficient of the first mode ζ_1	0.00185

2.2 Design of the semi-active oil damper

A semi-active oil damper is designed using two solenoid valves, which have different orifice diameters, 3 mm and 5 mm, so that it is able to switch the damping coefficient of the damper to four stages. To derive the damping coefficients of the damper, force-displacement relationships are measured. Figure 2 shows the force-displacement curves. Based on the area of the ellipses surrounded by the curves, the four stages of damping coefficients are obtained as shown in Table 2.

Table 2: Damping coefficients of the semi-active oil damper

	Damping coefficient [$\times 10^{-2}$ Ns/mm]
c_{s_1}	3.08
c_{s_2}	4.01
c_{s_3}	4.45
c_{s_4}	8.48

3 DESIGN OF THE CONTROL SYSTEM

3.1 Equations of motion

The equation of motion of the model can be written with $\boldsymbol{x} = [x_1, x_2]^{\mathrm{T}}$ as

$$\mathbf{M}\ddot{\boldsymbol{x}} + \mathbf{C}\dot{\boldsymbol{x}} + \mathbf{K}\boldsymbol{x} = \mathbf{E}u + \mathbf{F}\ddot{x}_0 \tag{5}$$

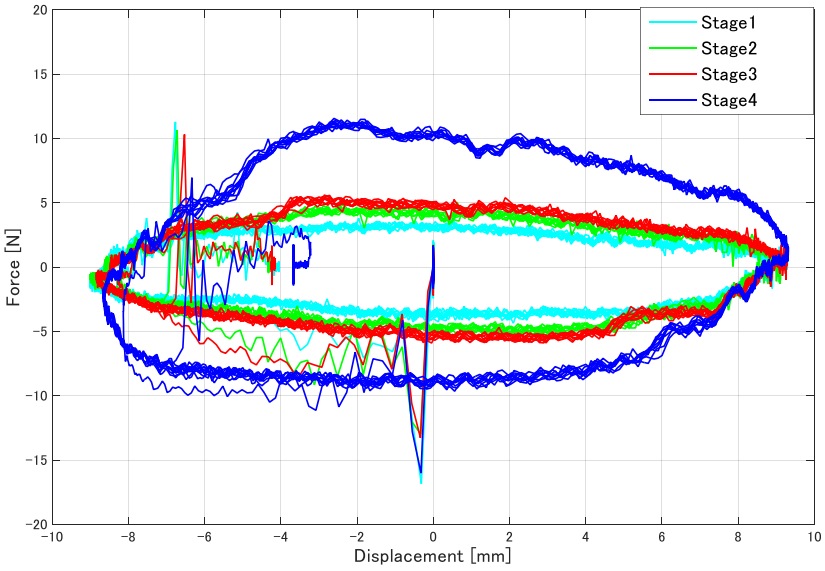

Figure 2: Displacement-force curves of the semi-active oil damper

where

$$\mathbf{E} = \begin{bmatrix} 1 \\ 0 \end{bmatrix}, \mathbf{F} = -\begin{bmatrix} m_1 \\ m_2 \end{bmatrix} \tag{6}$$

and u is the control force given by the semi-active oil damper. From these equations, a state space equation can be written as

$$\dot{\mathbf{X}} = \mathbf{A}\mathbf{X} + \mathbf{B}u + \mathbf{G}\ddot{x}_0 \tag{7}$$

where

$$\mathbf{A} = \begin{bmatrix} \mathbf{O} & \mathbf{I} \\ -\mathbf{M}^{-1}\mathbf{K} & -\mathbf{M}^{-1}\mathbf{C} \end{bmatrix}, \mathbf{B} = \begin{bmatrix} \mathbf{0} \\ -\mathbf{M}^{-1}\mathbf{E} \end{bmatrix}, \mathbf{G} = \begin{bmatrix} \mathbf{0} \\ -\mathbf{M}^{-1}\mathbf{F} \end{bmatrix} \tag{8}$$

and $\mathbf{X}$ is the state vector written as

$$\mathbf{X} = \begin{bmatrix} \boldsymbol{x} \\ \dot{\boldsymbol{x}} \end{bmatrix}. \tag{9}$$

3.2 Power-law damping

Based on the power-law damping control system, the optimal control force u in equation (5) is represented by the nonlinear cubic damper c_3 as

$$u = c_3 \dot{x}_1^{\,3} \tag{10}$$

and $1.0\times10^3\mathrm{Ns}^3/\mathrm{m}^3$ and $1.5\times10^3\mathrm{Ns}^3/\mathrm{m}^3$ are selected as the two possible values of the damping coefficient c_3 of the nonlinear damper in this study. Using the optimal control force u and Table 2, the actual control force u_{real} can be written as equation (11).

$$u_{\mathrm{real}} = \begin{cases} c_{\mathrm{s}_1}\dot{x}_1 & (-u/\dot{x}_1 < c_{\mathrm{d}_1}) \\ c_{\mathrm{s}_2}\dot{x}_1 & (c_{\mathrm{d}_1} < -u/\dot{x}_1 < c_{\mathrm{d}_2}) \\ c_{\mathrm{s}_3}\dot{x}_1 & (c_{\mathrm{d}_2} < -u/\dot{x}_1 < c_{\mathrm{d}_3}) \\ c_{\mathrm{s}_4}\dot{x}_1 & (c_{\mathrm{d}_3} < -u/\dot{x}_1) \end{cases} \tag{11}$$

where

$$\begin{aligned} c_{\mathrm{d}_1} &= \frac{c_{\mathrm{s}_1} + c_{\mathrm{s}_2}}{2}, \\ c_{\mathrm{d}_2} &= \frac{c_{\mathrm{s}_2} + c_{\mathrm{s}_3}}{2}, \\ c_{\mathrm{d}_3} &= \frac{c_{\mathrm{s}_3} + c_{\mathrm{s}_4}}{2}. \end{aligned} \tag{12}$$

4 RESULTS OF SHAKING-TABLE TESTS

In order to verify the effectiveness of the power-law damping control system, four cases of shaking-table tests are conducted. The settings of the tests are shown in Table 3. Random vibrations are used as input excitations and 10 times tests are conducted for each setting.

Table 3: Settings of shaking-table tests

Code	Control system
NC	No controller (passive damper)
LQG	Linear-quadratic-Gaussian control
PLD1	Power-law damping control ($c_3 = 1.0 \times 10^3[\mathrm{Ns}^3/\mathrm{m}^3]$)
PLD2	Power-law damping control ($c_3 = 1.5 \times 10^3[\mathrm{Ns}^3/\mathrm{m}^3]$)

Figures 3 (a) to 3 (d) show examples of the acceleration transmissibility of the 1st and 2nd floors. Here, the acceleration transmissibility of the i-th floor can be obtained by

$$T_i(\Omega) = \frac{|F[\ddot{x}_i(t) + \ddot{x}_0(t)]|}{A} \tag{13}$$

where $F[\cdot]$ represents the Fourier transform operation and A is the maximum amplitude of the input excitation.

Compared with LQG control, power-law damping with $c_3 = 1.0 \times 10^3\mathrm{Ns}^3/\mathrm{m}^3$ (PLD1) as shown in Figure 3 (c) can reduce the acceleration transmissibility of the system in resonant

frequency range but not affect the performance out of the resonant range. However, the power-law damping with $c_3 = 1.5 \times 10^3 \mathrm{Ns}^3/\mathrm{m}^3$ (PLD2) has worse results compared with PLD1 as shown in Figure 3 (d), so that it can be concluded that it is important to select an appropriate value of c_3.

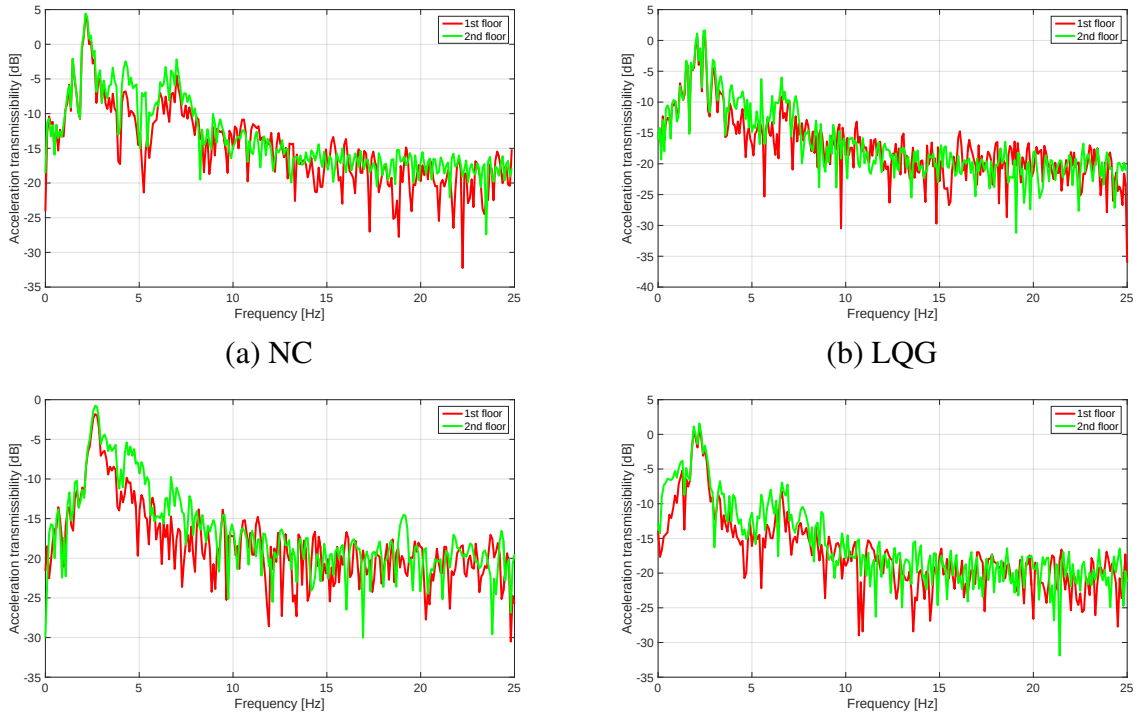

(a) NC (b) LQG

(c) PLD1 (d) PLD2

Figure 3: Examples of the acceleration transmissibility

Figures 4 (a) and (b) show the average of the maximum values of the acceleration transmissibility of the 1st and 2nd floors over 10 times tests of each setting. From these results, It can be observed that PLD1 has more robustness than other cases and would give a great performance against wide ranges of excitations.

Figures 5 (a) and (b) show the average of the maximum values of the absolute acceleration response of the 1st and 2nd floors. Each result is normalized as the maximum of the absolute value of the input excitation to one. It can be confirmed that PLD1 has more robustness than other control methods. However, PLD2 has worse results compared with LQG, therefore, it demonstrate again that the selection of the value of c_3 is very important in the power-law

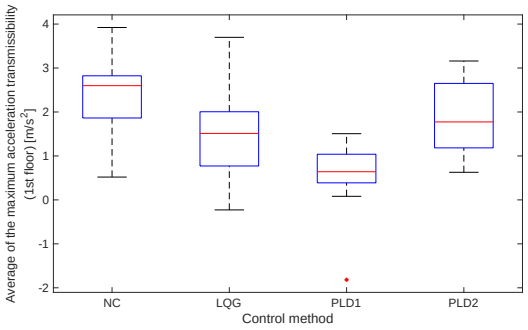

(a) 1st floor

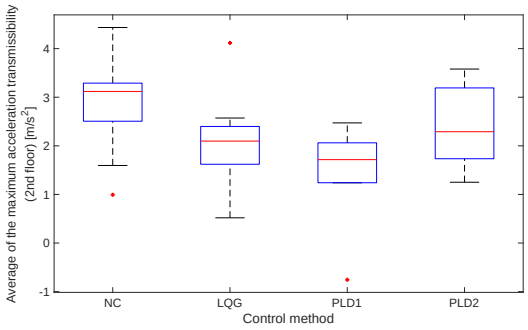

(b) 2nd floor

Figure 4: Average of the maximum values of the acceleration transmissibility

damping control system.

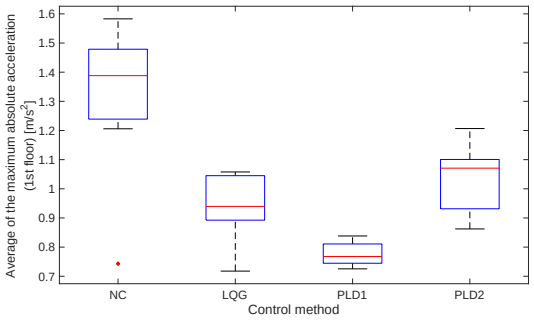

(c) 1st floor

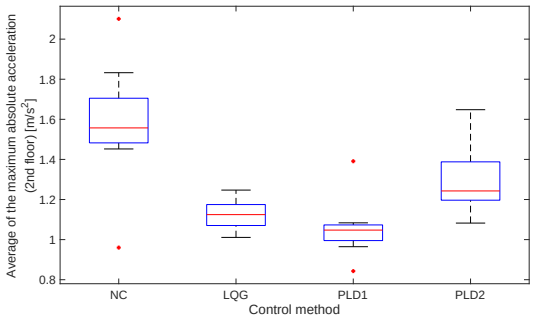

(d) 2nd floor

Figure 5: Average of the maximum values of the absolute acceleration response

5 CONCLUSIONS

In this study, shaking-table tests on a small-scale two-story physical building model are conducted in order to verify the effectiveness of a proposed power-law damping system. Through the shaking-table test, it is confirmed that power-law damping system can reduce the acceleration transmissibility of the system over resonant frequency range but not affect the performance out of the resonant range. However, the performance of the power-law damping control would decrease in case that the damping coefficient of the nonlinear damper (in this study, c_3) is not

selected appropriately. Therefore, an appropriate selection of c_3 has to be investigated for a future work.

ACKNOWLEDGEMENTS

This research was financially supported by the Japan Society for Promotion of Science KAKENHI Grant-in-Aid for Scientific Research (B) 24360230 and 16H04455. Also, the authors would like to acknowledge the Support of UK Royal Society for this work.

REFERENCES

[1] Dan, M., Ishizawa, Y., Tanaka, S., Nakahara, S., Wakayama, S., & Kohiyama, M. Vibration characteristics change of a base-isolated building with semi-active dampers before, during, and after the 2011 Great East Japan earthquake, *Earthquake and Structures*, **8**(4):889–913, 2015.

[2] Lang, Z., Guo, P., & Takewaki, I. Output frequency response function based design of additional nonlinear viscous dampers for vibration control of multi-degree-of-freedom systems, *Journal of Sound and Vibration*, **332**(19):4461–4481, 2013.

[3] Fujita, K., Kasagi, M., Lang, Z.-Q., Penfei, G., & Takewaki, I. Optimal placement and design of nonlinear dampers for building structures in the frequency domain, *Earthquakes and Structures*, **7**(6):1025, 2014.